# INFRASOUND SCALING AND ATTENUATION RELATIONS FROM SOVIET EXPLOSION DATA AND INSTRUMENT DESIGN CRITERIA FROM EXPERIMENTS AND SIMULATIONS

Jeffry L. Stevens, David A. Adams, G. Eli Baker, Heming Xu, and John R. Murphy,
Maxwell Technologies, Systems Division
Igor Divnov, V. N. Bourchik, and Ivan Kitov, Institute for the Dynamics of the Geospheres, Moscow, Russia

Sponsored by U. S. Department of Defense
Defense Threat Reduction Agency
Contract No. DSWA01-97-C-0129

**ABSTRACT**

This project has two distinct parts:

1. modeling of infrasound signals from atmospheric explosions and evaluation of International Monitoring System network performance using data from historic Russian nuclear tests and other infrasound data sources; and
2. analysis of infrasound instrumentation through a program of experimentation and theoretical modeling.

The Institute for the Dynamics of the Geospheres (IDG) in Moscow, Russia, has an archive of infrasound recordings from Soviet atmospheric nuclear tests that were conducted in 1957 and 1961, and has recently digitized the highest quality records from this data set. We have measured the infrasound signals from these records and compared them with previously developed scaling and attenuation relations. We find that the data are in best agreement with a scaling and attenuation relation developed by Los Alamos National Laboratory (LANL) which can be written as

$$\log P = 3.37 + 0.68 \log W - 1.36 \log R$$

where P is zero to peak pressure amplitude in Pascals, W is the yield in kilotons, and R is the source-to-receiver distance in kilometers. We use the scaling relations to define an infrasound magnitude, and to estimate the detection capability of the International Monitoring System (IMS) being developed as part of the Comprehensive Nuclear-Test-Ban Treaty (CTBT). Network capability is predicted using the network simulation programs NetSim and XNICE. The detection threshold for the proposed 60-station IMS network is estimated to be slightly higher than the design goal of 1 kT required by the CTBT.

We have developed the capability to numerically simulate the response to infrasound signals and a variety of noise models, of an arbitrary arrangement of porous hoses or of pipes with acoustic inlets. We performed experiments to assess different physical models of signal propagation in a cylindrical conduit to determine an appropriate basis for the model. The experiments also provide data for comparison with simulation results. We have run a series of simulations to assess the effect of different parameters on signal propagation, and to assess the performance of different instrument configurations in improving signal-to-noise ratios.

**Key Words**: infrasound, scaling relation, attenuation, atmospheric explosion, instrument

## OBJECTIVE

The objective of this project is to develop a better understanding of infrasound excitation, propagation, and recording in order to be able to predict the capability of the IMS network to detect and identify atmospheric explosions. To accomplish this, we are gathering a data set of infrasound recordings from historical Soviet explosions, modeling these data and using them to develop improved scaling and attenuation relations. In addition, we are using experimental and numerical methods to model the response of infrasound recording instrumentation.

## RESEARCH ACCOMPLISHED

### Part 1: Infrasound scaling and attenuation relations and IMS detection capability

The International Monitoring System (IMS) required by the Comprehensive Nuclear Test Ban Treaty (CTBT) will include sixty infrasound stations designed to detect atmospheric nuclear explosions. A design requirement is that the system be able to detect and locate explosions as small as one kiloton anywhere in the world. In order to estimate the capability of the infrasound network, it is necessary to be able to predict the amplitude of an infrasound signal at any location, and to evaluate whether the signal would be detectable above noise levels. In this paper, we use a data set of infrasound recordings from a set of Soviet explosions to put constraints on infrasound scaling relations and to estimate the detection capability of the IMS.

Scaling and attenuation relations are empirical and/or theoretical equations that relate the amplitude and period of infrasound signals to the explosion yield and source to receiver distance. Several different relations have been developed based on theoretical infrasound modeling, and on recordings of atmospheric nuclear and chemical explosions. We examine scaling and attenuation relations from Pierce and Posey (1971), Clauter and Blandford (1998), Whitaker (1995), and a set of relations derived by Russian scientists described by Stevens et al (1998). These scaling relations can be written as:

$\log P = -154 + \log W - 05 \log(R \sin \Delta)$ Pierce and Posey (1971) (1)

$\log P = 092 + 05 \log W - 147 \log \Delta$ AFTAC (Clauter and Blandford, 1998) (2)

$\log P = 337 + 068 \log W - 136 \log R$ LANL (Whitaker, 1995) (3)

$\log P = 300 + 033 \log W - \log R$ Russian – Crosswind (4)

$\log P = 330 + 033 \log W - \log R$ Russian – Downwind (5)

where P is zero to peak pressure in Pascals, W is yield in kilotons, R is distance in kilometers, and $\Delta$ is distance in degrees. The LANL relation uses a wind-corrected pressure.

The different scaling relations predict very different detection thresholds. Yield estimates for the threshold pressure level differ by several orders of magnitude, even though each relation was constrained by some infrasound data set. Table 1 shows the calculated yield at a nominal detection threshold of 0.1 Pascal for each of the scaling relations. The most important factor is the exponent in the pressure/yield relation. With the Pierce/Posey relation, which has a yield exponent of 1, pressure drops off much more rapidly with yield than with the other relations leading to a very high threshold level. The 0.33 yield exponent in the Russian relations, however, implies a very slow decrease in pressure with yield and leads to very low threshold levels. The Whitaker and Clauter/Blandford relations, which have yield exponents of 0.68 and 0.5, respectively, predict intermediate threshold levels.

| | 10 | 20 | 30 | 40 | 50 | 60 |
|---|---|---|---|---|---|---|
| Clauter/Blandford | 0.13 | 0.97 | 3.2 | 7.4 | 14 | 24 |
| Whitaker | 0.46 | 1.8 | 4.2 | 7.4 | 11 | 17 |
| Russia Crosswind | 0.0014 | 0.01 | 0.037 | 0.088 | 0.17 | 0.30 |
| Russia Downwind | 0.0002 | 0.0014 | 0.0046 | 0.011 | 0.02 | 0.037 |
| Pierce/Posey | 47 | 93 | 140 | 180 | 220 | 260 |

**Table 1.** Detection capability for a nominal detection threshold of 0.1 Pascal. The table shows yield in kilotons for each scaling relation and source to receiver distances from 10-60 degrees.

**Soviet Infrasound Data**

The Institute for the Dynamics of the Geospheres (IDG) in Moscow, Russia, has an archive of approximately 300 recordings from 34 Soviet atmospheric nuclear tests that were conducted in 1957 and 1961. 20 of these explosions were located at the Novaya Zemlya test site, 12 at Semipalatinsk, and 2 at Kapoustin Yar (see Figure 1). Of these, 178 recordings from 15 of the tests recorded at stations from 1000 to 5000 km were found to be of adequate quality for analysis. The yields of these tests range from 8 KT to 58 MT. IDG has digitized 65 of these waveforms to date. The data set includes one high altitude explosion and the largest atmospheric explosion ever detonated. The explosions corresponding to this data set are listed in Table 2. The number of records listed in the table is the number of records digitized. There are additional waveforms from several of the explosions that will be digitized at a later date. Paths to 17 recording stations are also shown on Figure 1.

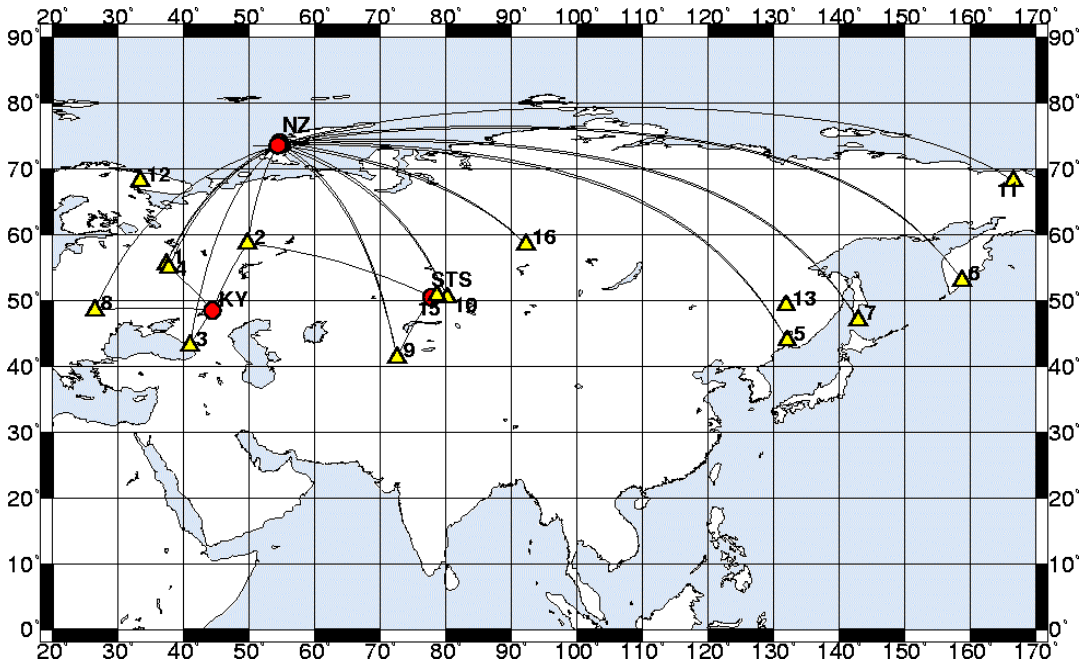


**Figure 1.** Stations recording infrasound signals from atmospheric explosions at three Soviet nuclear test sites Semipalatinsk (STS), Kapoustin Yar (KY), and Novaya Zemlya (NZ).

| Test Site | Explosion Number | Date | Time (Moscow) | Latitude | Longitude | Height of Burst (m) | Yield (KT) | Number of Records |
|---|---|---|---|---|---|---|---|---|
| STS | 088 | 09/04/61 | 08:00:27 | 50.45 | 77.74 | 730 | 7-9 | 2 |
| STS | 089 | 09/05/61 | 09:00:05 | 50.45 | 77.74 | 710 | 12-16 | 3 |
| KY | 091 | 09/06/61 | | 48.45 | 44.30 | 20000 | 10-11 | 6 |
| NZ | 095 | 09/10/61 | 12:00:14 | 73.52 | 54.30 | 2500 | 2400 | 23 |
| NZ | 116 | 10/02/61 | 13:30:50 | 73.92 | 54.55 | | 250-330 | 13 |
| NZ | 125 | 10/20/61 | 11:07:03 | 73.52 | 54.30 | | 1450 | 16 |
| NZ | 133 | 10/30/61 | 11:33:27 | 73.52 | 54.30 | 3500 | 58000 | 2 |

**Table 2.** Soviet atmospheric nuclear explosions and the number of records for each event that are currently being digitized. STS is the Semipalatinsk test site, KY is Kapoustin Yar, and NZ is Novaya Zemlya.

**Measurement of Russian data**

All of the Russian data were carefully measured in a consistent manner. The data were first filtered to remove long and short period noise outside the frequency band of the data. A Butterworth filter was used with corner frequencies of .01 and .2 Hz for events with yield less than 100 kilotons, .002 and .1 Hz for events with yields between 100 kilotons and 2 megatons, and .001 and .1 Hz for events with yield greater than 2 megatons. The amplitude and period were measured as half the maximum peak to peak amplitude and twice the time difference between the peak and trough, respectively. Measurements were made on both the acoustic wave and the low

frequency Lamb wave if possible. Only data with known instrument responses were measured, and a digital correction for the instrument response was made at the observed period.

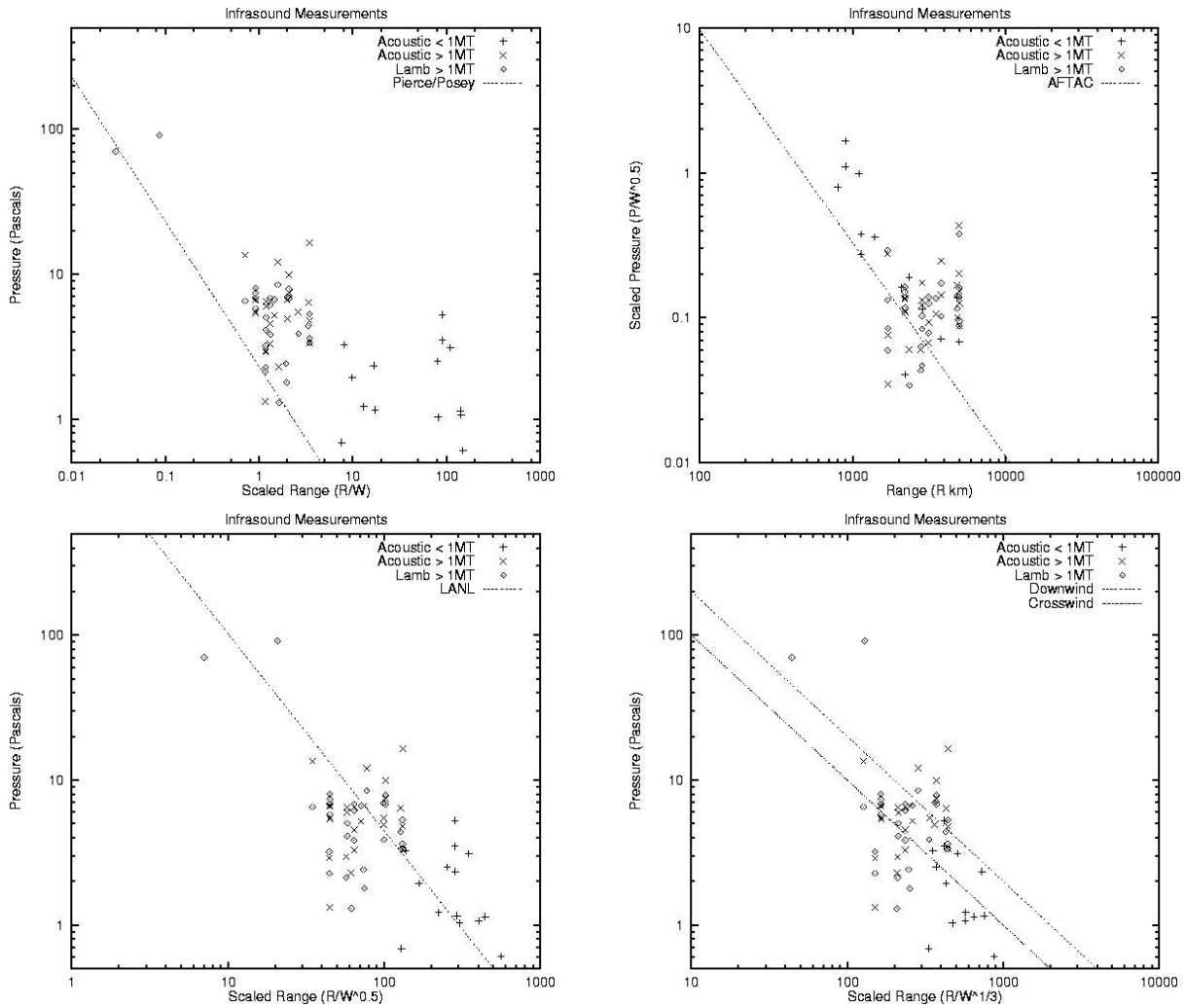


**Figure 2.** Comparison of Russian data with scaling relations. Top left is the Pierce/Posey relation equation 1, top right the AFTAC relation (Clauter and Blandford) equation 2, bottom left is the LANL relation (Whitaker) equation 3, and bottom right are the Russian relations equations 4 and 5.

Figure 2 shows a comparison between pressure measurements made from the Russian data and equations 1-5. It is not possible to put them all on the same plot because the scaling relations have different functional forms. The AFTAC relation (equation 2) fits the lower yield data and some of the higher yield data quite well. The Pierce/Posey relation (equation 1) is a fairly good fit to the high yield Lamb wave data, but does not fit the acoustic wave data, particularly for the lower yield events. The LANL relation (equation 3) appears to fit the data very well over the entire scaled range, although there is considerable scatter about the line. The pressure measurements have not been wind corrected since we do not have information about wind conditions at the time of the tests. The Russian relations (equations 4-5) also fit the data fairly well with the crosswind equations matching the lower amplitude data and the downwind equations matching the higher amplitude data, however the observed data falls below the predicted curves for larger scaled ranges, and the data points for the largest yield events are well above the curve, while the lower yield events lie below the curve. This suggests that the pressure/yield slope of 0.33 is too small.

The LANL relation has recently been adopted as the basis for an infrasound magnitude by the International Data Center (IDC) (Brown, 1999). The magnitude equation is $M_i = \log_{10} P + 136 \log_{10} R - 0019\,\nu$ where $\nu$ is stratospheric wind velocity in m/sec. Infrasound magnitudes for the Russian data set (without wind correction),

were calculated for the seven Soviet explosions. In calculating these magnitudes, we used the largest of the Lamb and acoustic arrival if both were measured. Figure 3 shows $M_i$ plotted vs. yield. Also shown is the LANL relation, equation 3, rewritten as a magnitude/yield relation $M_i = 068 \log W + 337$ . This equation fits the data over this very wide yield range very well. The exception is the high altitude explosion at Kapoustin Yar which lies above the curve by about 0.5 magnitude units.

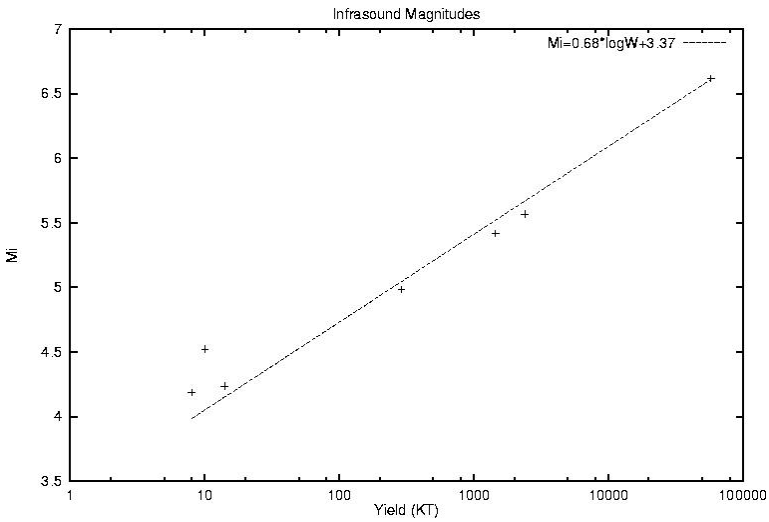


**Figure 3.** Infrasound magnitude plotted vs. yield for seven Soviet explosions.

**Spectral Measurements**

Some additional insight into the scaling laws can be obtained by examining the spectra of arrivals with different yields at the same station. Station 7, at Yuzno-Sakhalinsk, recorded four atmospheric explosions with yields of 250, 1450, 2400, and 58000 kilotons. The spectra of these four arrivals are shown in Figure 4. The shape of the spectra change dramatically over this yield range, with much more low frequency energy at higher yields.

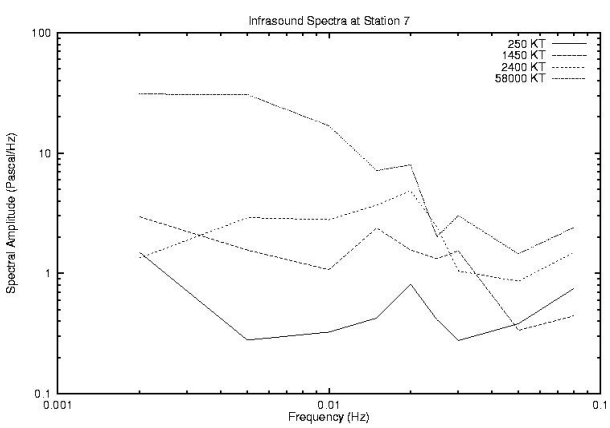


**Figure 4**. Spectra of four infrasound signals recorded at station 7 with yields of 250, 1450, 2400, and 58000 kilotons.

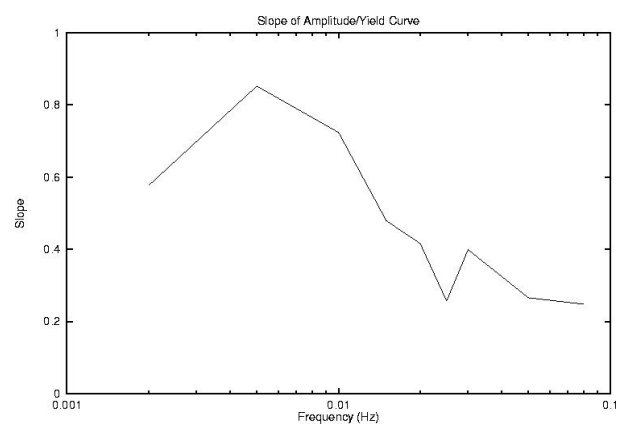


**Figure 5.** The slope of the log amplitude vs. log yield curve plotted as a function of frequency.

Figure 5 shows the slope of the amplitude vs. yield curve plotted as a function of frequency. This figure shows that the slope of the amplitude/yield curve is strongly frequency dependent, and that the slope is close to 1, as in the Pierce/Posey model, at very low frequencies, but declines to approximately 1/3, as in the Russian scaling laws, at higher frequencies.

**Network Detection Simulations**

In order to predict the performance of the proposed 60 station IMS infrasound network, we modified the network simulation program NetSim (Sereno et al., 1990) to include the models of infrasound propagation described in equations 10-14. NetSim uses these equations to calculate the pressures as a function of yield and range. These are used together with station locations, a noise model, a minimum signal to noise ratio for reliable measurement, and the number of stations required for a signal to be reported, to determine the network detection threshold as a function of position on the earth. We have calculated detection thresholds for the proposed IMS network under the following assumptions:

1. Noise estimates were taken from Blandford and Clauter (1995). The amplitude of background noise is log normally distributed with log mean value of –1.1 (Pascals) and log standard deviation of 0.33. The noise distribution is taken to be geographically uniform.
2. The minimum signal to noise ratio for detection is 2.
3. Two stations detect infrasound signals at a 90% confidence level.
4. Four element infrasound arrays increase signal to noise ratio by a factor of 2.
5. Propagation error has a log standard deviation in log signal of 0.2.

Detection threshold maps were calculated for the AFTAC and LANL scaling relations. We did not calculate the detection threshold for the Pierce Posey or Russian models because they are clearly unrealistic for yields near the detection threshold. The results are shown in Figures 6-7. For the LANL models, the detection threshold is predicted to be between 0.7 and 3.2 kilotons depending on location. For the AFTAC model, the detection threshold is between 0.3 and 2.3 kilotons. Since other factors are uniform in these simulations, the variations in threshold level are determined by station coverage. These scaling relations with the conditions listed above predict, therefore, that the infrasound detection threshold for the IMS network is somewhat higher than the design goal of one kiloton, and that explosions near this limit could escape detection at some locations.

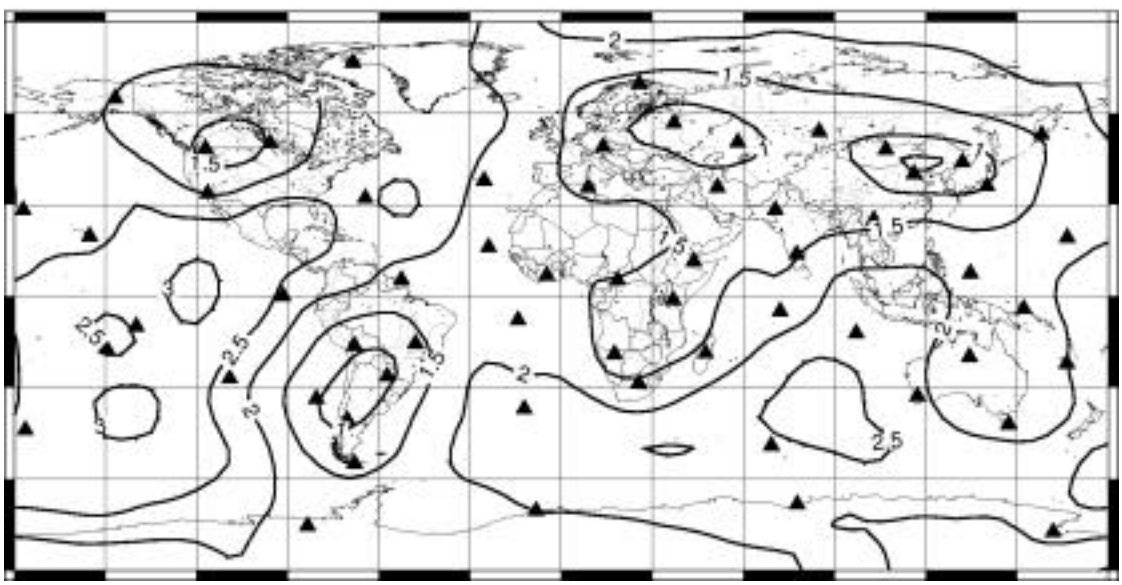


**Figure 6.** Contours showing detection thresholds with a 90% level of confidence for detection at 2 infrasound stations. The intervals are logarithmically spaced with labels in kilotons. The model is from Whitaker (1995).

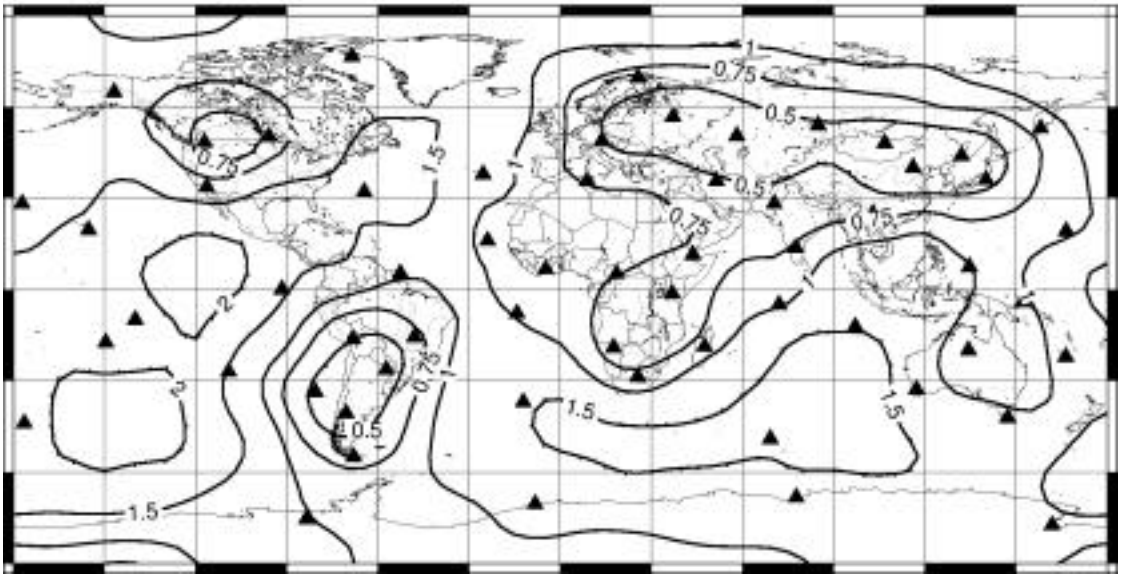


**Figure 7.** Contours showing detection thresholds with a 90% confidence level for detection at 2 infrasound stations. The intervals are logarithmically spaced with labels in kilotons. The model is from Clauter and Blandford (1998).

## Part 2: Infrasound instrumentation research

The goal of the instrumentation work is the accurate simulation of the response of any configuration of pipes and inlets used as a spatial filter for a microbarograph. Such a capability will enable the optimization of instrument designs and the separation of instrument from source and propagation effects. Initial experiments performed to ensure that the simulations have a valid physical basis are described in Stevens et al (1998). Additional experiments are described below. We also describe the numerical method used to perform the simulations, present results of simulations that compare the performance of different configurations, and discuss the remaining experimental and theoretical work that must be performed.

We measured the dispersion of infrasound signals between approximately 0.1 and 10 Hz at amplitudes of 1 to 5 Pascals, the typical range for infrasound signals (Figure 8). These results are consistent with the physical model of acoustic wave propagation in a cylindrical conduit, which provides the basis for our numerical model.

No proposed physical models that we have considered accurately predict attenuation. This lack of a theoretical understanding of the attenuation requires that the model use an empirically determined exponential decay factor for acoustic wave propagation in a cylindrical conduit. Furthermore, to provide meaningful and accurate numerical simulations, the attenuation of each material used to construct spatial filters must be determined empirically.

The numerical simulations use a propagator method, developed and detailed by Burridge (1971), to obtain the pipe response. The flux-pressure vector $\begin{pmatrix} f \\ p \end{pmatrix}$ is propagated through an impermeable section of pipe of length $l$ by

$$\begin{pmatrix} f(x+l) \\ p(x+l) \end{pmatrix} = \begin{pmatrix} \cosh \Gamma l & -\frac{1}{Z_0} \sinh \Gamma l \\ Z_0 \sinh \Gamma l & \cosh \Gamma l \end{pmatrix} \begin{pmatrix} f(x) \\ p(x) \end{pmatrix} = M \begin{pmatrix} f(x) \\ p(x) \end{pmatrix}, \tag{6}$$

where $p(x)e^{i\omega t}$ is a harmonic pressure fluctuation and $f(x)e^{i\omega t}$ is a harmonic volume flux at a distance x from the left end of the pipe. $\Gamma$ and $Z_0$ are the propagation constant and characteristic impedance of the pipe, both dependent in a complicated way upon frequency, radius of the pipe, and other variables (Burridge, 1971; Benade, 1939). The resulting flux-pressure vector from an inlet at x with impedance $Z_k$ is propagated by

$$\begin{pmatrix} f(x_+) \\ p(x_+) \end{pmatrix} = \begin{pmatrix} 1 & -\frac{1}{Z_k} \\ 0 & 1 \end{pmatrix} \begin{pmatrix} f(x_-) \\ p(x_-) \end{pmatrix} + \begin{pmatrix} Pe_k / Z_k \\ 0 \end{pmatrix} = N \begin{pmatrix} f(x_-) \\ p(x_-) \end{pmatrix} + \begin{pmatrix} Pe_k / Z_k \\ 0 \end{pmatrix} \tag{7}$$

where, $x_\pm$ are the right and left side of the location $x$, and $Pe$ is the pressure disturbance at the inlet. Therefore, the flux-pressure vectors at $x_1$ and $x_2$, two locations along the pipe, are related by

$$\begin{aligned} \begin{pmatrix} f(x_2) \\ p(x_2) \end{pmatrix} &= M_{Nb+1} \prod_{i=Nb}^{1} N_i M_i \begin{pmatrix} f(x_1) \\ p(x_1) \end{pmatrix} + M_{Nb+1} \left[ \begin{pmatrix} Pe_{Nb} / Z_{Nb} \\ 0 \end{pmatrix} + \sum_{j=2}^{Nb} \prod_{i=Nb}^{j} N_i M_i \begin{pmatrix} Pe_{j-1} / Z_{j-1} \\ 0 \end{pmatrix} \right] \\ &= A \begin{pmatrix} f(x_1) \\ p(x_1) \end{pmatrix} + B \end{aligned} \tag{8}$$

where $Nb$ is the number of inlets between $x_1$ and $x_2$, the inlets are numbered as 1, 2, …, $Nb$ from $x_1$ and $x_2$, $N$'s are the propagator matrices at the inlets, $M_1$, $M_{Nb+1}$ as defined in equation (6) correspond to the propagator matrices between $x_1$ and the first inlet and between $x_2$ and the last inlet, $M_k, k=2,Nb$ are the propagator matrices between the k'th and (k+1)'th inlets, and A and B are the propagator matrices from $x_1$ and $x_2$. The method is extended to derive the response of multiple pipe arrays.

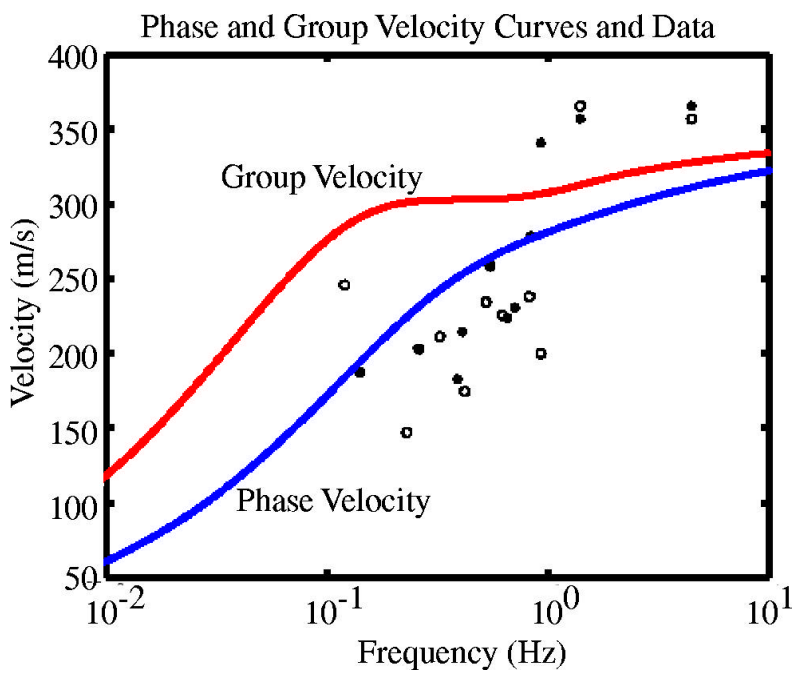


Figure 8: Theoretical dispersion curves for acoustic waves in cylindrical conduits (from Haak and de Wilde, 1998), and group velocity measurements.

Three configurations used to reduce noise interference are considered (Figure 9). One is a simple 20 m radius star system, in which several identical pipes with inlets join at the center. The second is a 30 m star with the inner 10 m of each pipe impermeable, to reduce the effect of spatially correlated noise. The last is a hexagonal system, in which the 20 m transverse pipes are composed of pipes with inlets and the 20 m radial pipes are impermeable.

For the star receiver system, we compute the pressure response for a few cases. Figure 10 (left) shows that the response to a vertically propagating signal varies with the length of the pipe. The number of inlets in each pipe is held constant. The response is nearly flat at lower frequency, decreases in the intermediate frequency range, but exhibits peaks corresponding to the resonance frequencies of the pipe. The decay at higher frequencies is associated with the increase of the propagation constant in the pipe. To avoid resonant peaks in the frequencies of interest, the pipe length will be limited. For CTBT monitoring from 0.01 to 4 Hz, the maximum length is approximately 30 meters. For pipes of the same length the response varies with the number of the inlets, as shown in Figure 10 (right) for the case of vertical incidence. Using more inlets flattens the response curve at

higher frequencies and thus increases the bandwidth. At still higher frequency the signal decays rapidly and is interfered with by resonance peaks. The response is similar for the hexagonal configuration.

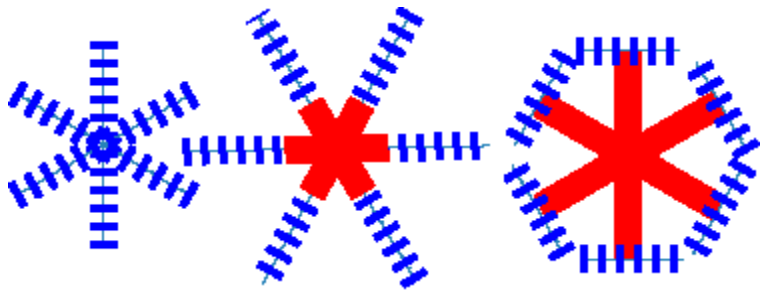

Figure 9: Dashed lines represent pipes with 100 acoustic ohm inlets at 1 meter spacing. Solid lines represent impermeable pipes. The pressure is measured in the center of each configuration.

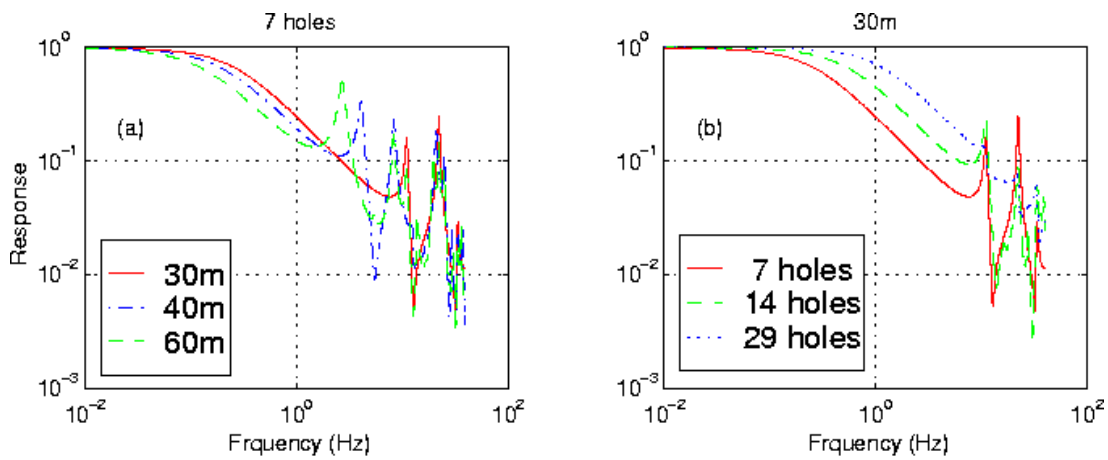


Figure 10: Response of star pipe systems of different lengths (left) and number of inlets (right).

The advantage one configuration has over another will likely occur in its noise suppression characteristics. The permeable pipes are in different locations relative to the center of the two configurations, and the noise, mainly from wind, may correlate over some length, so the systems examined may exhibit different noise reduction capabilities. This may be offset by the greater loss in signal amplitude for configurations in which the signal must propagate further. We use Gaussian noise with 0, 2, 5, and 10 meter correlation lengths to simulate infrasonic noise and assess noise reduction, which is much greater for less well-correlated noise for each configuration (e.g. Figure 11, left). There is little enhancement of S/N by any of the configurations, for 10 and 5 m correlation length noise, while for the uncorrelated and 2 m correlation length noise, there is significant improvement in S/N, and better performance by both of the star configurations.

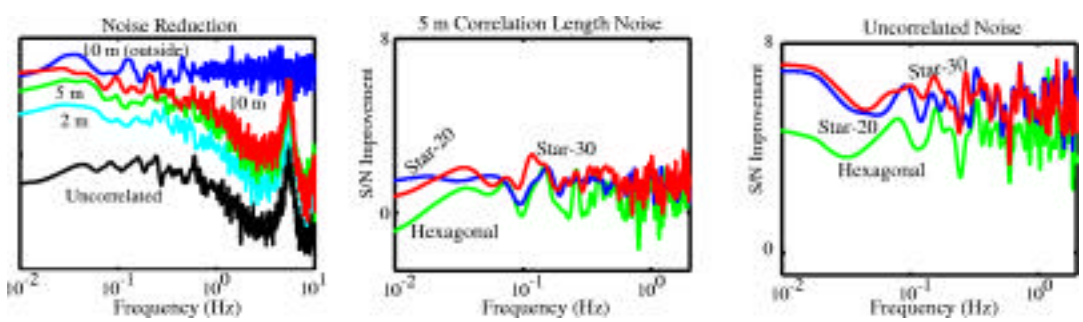


Figure 11: At left are noise spectra before (upper spectral line) and after spatial filtering by a 30 m star configuration (Figure 9, center) for 10m, 5m , 2m, and uncorrelated noise (successively lower spectral lines). Input frequency spectra are flat and the same amplitude for each noise type. The increase in S/N for a vertically incident plane wave and 5 m correlation length noise (center), and uncorrelated noise (right), are shown for different configurations.

## CONCLUSIONS AND RECOMMENDATIONS

In the analysis above, we used a data set of infrasound waveforms from Soviet atmospheric tests ranging in yield from 8 kilotons to 58 megatons to place constraints on infrasound scaling relations and to estimate the detection threshold of the future International Monitoring System. Analysis of 42 waveforms shows that measured pressures are consistent with yield and attenuation scaling relations developed at LANL for HE tests, and also fairly consistent with a scaling relation developed by AFTAC. The scaling relations developed by Pierce and Posey are consistent with Lamb waves from very large explosions, but not with acoustic waves from smaller explosions.

The network simulation results indicate that the detection threshold of the future IMS infrasound network may be somewhat higher than the one-kiloton design goal. This result depends, of course, on a number of assumptions that went into the simulations. The most important of these is the background noise level. While we have used the same noise level worldwide, clearly the noise levels will vary depending on location. Blandford et al (1995) made threshold estimates using station dependent noise estimates derived from average wind values and found significantly lower threshold levels. The accuracy of the simulation could be improved considerably by using noise measurements gathered from each infrasound station location, a process which is still in its early stages. We also made the assumptions that a four element array leads to a factor of two improvement in signal/noise ratio, and that a signal can be identified with a signal to noise ratio of 2. Both of these assumptions are probably optimistic. Improvements could also be made in the signal modeling, particularly by including stratospheric winds, which will have the effect of improving detection in some directions and degrading it in others. Excitation and propagation, however, appear to be modeled quite well by the LANL relation, equation 3, over a wide range of explosion yields and distance ranges, and this relation can be used to predict infrasound amplitudes in network simulations.

Our experimental work confirms that acoustic waves in a cylindrical conduit provide an appropriate physical basis for numerical simulations of infrasound instrument response. We have developed an accurate and computationally efficient numerical model, which permits determination of the response of any pipe configuration. Three configurations tested show distinctly different S/N performance. Determination and incorporation of realistic noise models and empirical measures of attenuation for the particular materials used will be necessary to ensure that the simulations are relevant to instruments that will be deployed as part of the IMS. This will be the focus of future instrumentation efforts.

## REFERENCES

Benade, A. H., 1968, On the propagation of sound waves in a cylindrical conduit, *J. Acoust. Soc. Am.*, 2, 616-623.

Blandford, R. R. and D. A. Clauter (1995), "Capability Estimation of Infrasound Networks", AFTAC report.

Blandford, R. R., D. A. Clauter, R. W. Whitaker, and T. Armstrong (1995), "Infrasound Network Options," AFTAC/DOE White Paper presented at VMTF meeting.

Brown, D. J. (1999) "Summary of Infrasound Source Location Meeting: San Diego, November 9-10, 1998, Center for Monitoring Research Technical Report CMR-99/02, January.

Burridge, R., 1971, The acoustics of pipe arrays, *Geophys. J. R. Astroc. Soc.*, 6, 53-69.

Clauter, D. A. and R. R. Blandford (1998), "Capability Modeling of the Proposed International Monitoring System 60-Station Infrasonic Network," proceedings of the Infrasound workshop for CTBT monitoring, Santa Fe, New Mexico, August 25-28, 1997, LANL report number LA-UR-98-56.

Haak, H.W. and G.J. de Wilde (1998), "On the Propagation of Low Frequency Sound Waves in Porous Hoses used in Infrasound Detection Systems, pre-print

Pierce, A. D. and J. W. Posey (1971), "Theory of the Excitation and Propagation of Lamb's Atmospheric Edge Mode from Nuclear Explosions," *Geophys. J. R. astr. Soc.*, **26**, 341-368.

Sereno, T. J., S. R. Bratt, and G. Yee (1990), "NetSim: A computer program for simulating detection and location capability of regional seismic networks," SAIC Annual Technical Report to DARPA, SAIC 90/1163, March.

Stevens, J. L., G. E. Baker, J. R. Murphy, J. Morris, and I. I. Divnov (1998), "Infrasound Excitation and Propagation Research," Proceedings of the 20th Seismic Research Symposium on Monitoring a Comprehensive Test Ban Treaty, 21-23 September, 1998.

Whitaker, R. W. (1995), "Infrasonic Monitoring," proceedings of the 17th annual Seismic Research Symposium in Scottsdale, AZ, September 12-155, 1995, 997-1000.